Materials Science and Engineering C 33 (2013) 634–640

Contents lists available at SciVerse ScienceDirect

Materials Science and Engineering C

journal homepage: www.elsevier.com/locate/msec

Modified gold surfaces by 6-(ferrocenyl)hexanethiol/dendrimer/gold nanoparticles as a platform for the mediated biosensing applications

Murat Karadag [a], Caner Geyik [a], Dilek Odaci Demirkol [a], F. Nil Ertas [b], Suna Timur [a,*]

[a] Ege University, Faculty of Science, Biochemistry Department, 35100 Bornova-Izmir, Turkey
[b] Ege University, Faculty of Science, Chemistry Department, 35100, Bornova-Izmir, Turkey

ARTICLE INFO

Article history:
Received 9 May 2012
Received in revised form 14 September 2012
Accepted 26 October 2012
Available online 2 November 2012

Keywords:
Glucose biosensor
Gold nanoparticles
Self assembled monolayers

ABSTRACT

An electrochemical biosensor mediated by using 6-(Ferrocenyl) hexanethiol (FcSH) was fabricated by construction of gold nanoparticles (AuNPs) on the surface of polyamidoamine dendrimer (PAMAM) modified gold electrode. Glucose oxidase (GOx) was used as a model enzyme and was immobilized onto the gold surface forming a self assembled monolayer via FcSH and cysteamine. Cyclic voltammetry and amperometry were used for the characterization of electrochemical response towards glucose substrate. Following the optimization of medium pH, enzyme loading, AuNP and FcSH amount, the linear range for the glucose was studied and found as 1.0 to 5.0 mM with the detection limit (LOD) of 0.6 mM according to S/N = 3. Finally, the proposed Au/AuNP/(FcSH + Cyst)/PAMAM/GOx biosensor was successfully applied for the glucose analysis in beverages, and the results were compared with those obtained by HPLC.

© 2012 Elsevier B.V. All rights reserved.

1. Introduction

Glucose oxidase (GOx; β-D-glucose:oxygen 1-oxidoreductase; EC 1.1.3.4) is a dimeric protein containing one tightly bound flavin adenine dinucleotide (FAD) per monomer as cofactor, and catalyzes the oxidation of β-D-glucose to D-glucono-δ-lactone and hydrogen peroxide using molecular oxygen as the electron acceptor [1]. However, the thick protein layer surrounding flavin redox centre results in difficulties on direct electron transfer between FAD and electrodes [2,3]. It has taken about half a century and tremendous amount of research to overcome this problem and to obtain better electron transfer between the enzyme and electrodes such as adding redox mediators [4], conducting polymers [5], nanoparticles [6] and dendrimers [7]. The surface quality is an important factor affecting results obtained with electrochemical methods especially when self assembled monolayers (SAMs) are applied to build a recognition layer with various functional groups. SAMs of alkanethiols bearing different functional groups have been widely used in studies of the intelligent modification of solid surfaces. Alkanethiol SAMs having terminal electro-active groups were considered to be ideal for understanding the fundamentals of the electron transfer process at an electrode/solution interface and received a great deal of attention [8,9]. Among these electroactive groups, the ferrocenylalkanethiol monolayer has been used as a model system to study the electron exchange between ferrocenyl groups and gold electrodes, because of the simple and good electrochemical characters of the ferrocene groups [9]. 6-Ferrocenyl-1–hexanethiol ($Fc(CH_2)_6SH$; will be referred as FcSH) has been previously investigated as SAM to meet such purposes [8].

Nanoscale materials combined with biological components hold the potential of revolutionary changes in fields of science and technology [10]. There is rapidly increasing interest in nanotechnology in analytical chemistry [11] and clinical diagnosis [12,13]. The high surface to mass ratio makes nanomaterials exhibit unique physical and chemical properties [10,11,14,15]. Among these unique characteristics of nanomaterials, electronic properties are widely used to construct electrochemical biosensors. Gold nanoparticles (AuNPs) are mostly used metal-nanoparticles in the construction of enzymatic sensors [15]. Such works carried out by Sun and co-workers, have been reported to increase bioelectrocatalytic response in glucose biosensors [6,16,17]. Beside metallic nanoparticles, dendrimers as immobilization materials are also being used widely because of advantages such as biocompatibility, stability, porous structure and enlarging surface [18]. Polyamidoamine (PAMAM) provides abundant amine groups available for biomolecules immobilization.

Here, we described a mediated glucose biosensor based on Au/AuNP/(FcSH + Cyst)/PAMAM/GOx system and investigated the effect of the presence of AuNPs and FcSH. After optimization studies, analytical characterization experiments were carried out by amperometric measurements.

2. Materials and methods

2.1. Materials

Glucose oxidase (GOx; EC 1.1.3.4, 21200 units/g, type II-S, from *Aspergillus niger*), β-D-glucose (99.5%) purchased from Sigma (USA). 6-ferrocenyl-1-hexanethiol and polyamidoamine (PAMAM

* Corresponding author. Fax: +90 232 3438624.
E-mail address: suna.timur@ege.edu.tr (S. Timur).

0928-4931/$ – see front matter © 2012 Elsevier B.V. All rights reserved.
http://dx.doi.org/10.1016/j.msec.2012.10.008

G4 dendrimers in methanol solution) are obtained from Aldrich Chem. Co (USA). Sodiumborohydride (99%), glutaraldehyde solution (Grade II, 25%) and gold colloidal solution (10 nm, 0.75A_{520} units/mL, Concentration: ~0.01% as $HAuCl_4$) are purchased from Sigma-Aldrich. Cysteamine hydrochloride was purchased from Fluka. All other chemicals were analytical grade. Distilled and de-ionized water was used during experiments.

2.2. Apparatus

The electrochemical measurements were performed with a potentiostat (PalmSens, The Netherlands). A conventional three electrode system was used in experiments, namely: Ag/AgCl electrode as a reference (Metrohm, Switzerland), a platinum wire as an auxiliary electrode (BAS; United Kingdom, USA), and a gold electrode (BAS; United Kingdom, USA) as working electrode. During amperometric determinations, a magnetic stirrer and a stirring bar provided the desired convective transport in the reaction cell. Cyclic voltammetry was performed in quiescent solutions.

High-performance liquid chromatography (HP1100, Hewlett and Packard, Santa Clara, CA, USA) with a refractive index detector (RI) controlled by a HP-Chemstation from Agilent (Karlsruhe, Germany) was used as reference method for sample applications.

The morphology of modified gold surfaces with AuNP and AuNP/FcSH were imaged by Atomic Force Microscopy (AFM, NanoMagnetics Instruments, UK), at ambient temperature in non-contact mode.

2.3. Preparation of Au/AuNP/(FcSH + Cyst)/PAMAM/GOx Biosensor

The gold electrode surface was initially polished with alumina powder (Gamma, 0.05 lm) and was conditioned in 0.5 M H_2SO_4 solution by cycling the potential between 0 and +1.5 V until a reproducible voltammetric response was obtained. Then, the modification of the electrode was carried out by following the steps given in a previous study [19]. Briefly, the cleaned gold surface was immersed in cysteamine (100 mM) and 5.0 μL (1.98 μmol) of 6-ferrocenyl-1-hexanethiol solution in the mixture of acetonitrile and ethanol (ACN: EtOH; 1:1, v/v) for 30 min and washed with distilled water to get rid of physically adsorbed molecules. Then, dipped into glutaraldehyde solution (5.0%, v/v, in potassium phosphate buffer, pH 7.0; 50 mM) for 30 min and again washed with distilled water. After that, exposed to the solution of PAMAM dendrimer (1.0%, v/v) for 1 h, treated with 5.0 mM $NaBH_4$ for 30 min, and washed with distilled water [19]. 42 U of GOx (2.0 mg in 5.0 μL potassium phosphate buffer, pH 7.0; 50 mM), 5.0 μL of AuNPs solution and 5.0 μL of glutaraldehyde (1.0%, v/v) were added to electrode surface respectively. Then, surface was allowed to dry at 25 °C for about 30 min. The modified electrode was stored in contact with the working buffer solution when not in use. Schematic representation of thme preparation of Au/AuNP/(FcSH + Cyst)/PAMAM/GOx biosensor was shown in Scheme 1.

2.4. Electrochemical measurements

All amperometric measurements were carried out by applying a potential +0.35 V (vs. Ag/AgCl reference and Pt wire as counter electrode) at ambient temperature. 10.0 mL of working buffer solution (50 mM, pH 4.0 Na-Acetate buffer) was used in the voltammetric cell. The cell was rinsed with distilled water and the working buffer solution respectively after each measurement. In all amperometric measurements, the error bars on each plot represent the standard deviation of three replicates of the related measurement.

In order to investigate electron transfer properties of proposed system, cyclic voltammetry experiments were carried out in the presence and absence of AuNPs and FcSH. Obtained results from these different electrodes compared to characterize the effects of mediator and nanoparticles in the electrode configuration.

2.5. Sample application

In order to verify the performance and feasibility of the proposed Au/AuNP/(FcSH + Cyst)/PAMAM/GOx biosensor for analysis of glucose in real samples, the biosensor was applied to glucose analysis in some beverages such as cherry juice and fizzy with orange. The samples were analyzed without any dilution or treatment and added directly to the reaction cell described above (2.4 Electrochemical Measurements). Results were compared with HPLC as a reference method. HPLC column (GL Sciences Inc. Inertsil NH_2 5.0 μm (4.6 I.D × 250 mm), Japan) was used for the chromatographic separation of monosaccharides at 30 °C. Injection volume was 20 μL. The mobile phase was acetonitrile:water (3:1 v/v). The flow rate was 1.0 mL/min). Initially, a calibration curve for glucose was constructed in a concentration range of 0.5–5.0 mg/mL. After dilution with mobile phase and filtration through membrane filter (pore size: 0.20 μM) samples were applied to the column. Then glucose levels were calculated using the calibration plot.

3. Results and discussion

3.1. Characterization

There have been a number of demonstrations of the applications of SAMs based biosensors. Silanes and alkanethiols have been mostly used to prepare DNA and enzyme sensors based on SAMs. In addition, dendrimers of different numbers of branches were bound onto a gold surface via cysteamine to construct SAMs based enzyme sensor for the detection of different analytes such as glucose [18] and pesticides [20]. In this study, FcSH as a mediator and GOx were immobilized by means of PAMAM via construction of SAM via cysteamine. The use of glutaraldehyde as the cross-linker resulted in more stable enzyme immobilization. The enzymatic process occurs according to the following reaction:

$$\mathrm{Glucose} + \mathrm{GOx(FAD)} \rightarrow \mathrm{Gluconolactone} + \mathrm{GOx(FADH_2)}$$

$$\mathrm{GOx(FADH_2)} + 2\mathrm{AuNP/Cyst-HS-Fc^+} \rightarrow \mathrm{GOx(FAD)} + 2\mathrm{AuNP/Cyst-HS-Fc} + 2\mathrm{H^+}$$

$$\mathrm{AuNP/Cyst-HS-Fc} \rightarrow \mathrm{AuNP/Cyst-HS-Fc^+} + 2\mathrm{e^-}$$

where Fc represents reduced and oxidized forms in the redox layer, GOx(FAD) and GOx($FADH_2$) are the oxidized and reduced forms of GOx.

The electrochemical behaviour of the enzyme electrode was studied using cyclic voltammetry. Fig. 1 shows the cyclic voltammograms of the Au/AuNP/(FcSH + Cyst)/PAMAM/GOx in working buffer solution at different scan rates.

The peak at +0.35 V corresponds to the oxidation peak of FcSH. No reverse peak was obtained indicating the irreversible character of the electron transfer mechanism. The dependence of the peak currents on the scan rate as can be seen in Fig. 1 (inset). Peak currents linearly changes with the square root of scan rate, in the range from 5 to 100 mV/s, linear regression equation; $y = 0.123x - 0.059$, $R^2 = 0.998$ which indicates diffusion-controlled electrode process. It could be expected to obtain surface controlled system for monolayer immobilized material [21]. However, the transport of the substrate is controlled by diffusion from the solution. The presence of the dendrimer and bio-active layers upon an immobilized mediator might hinder this characteristic. Similar results have also been obtained in our previous work [22], which does not contain immobilized mediator. In the case of immobilized mediator forming SAMs, reversible character of PAMAM/enzyme layers is lost.

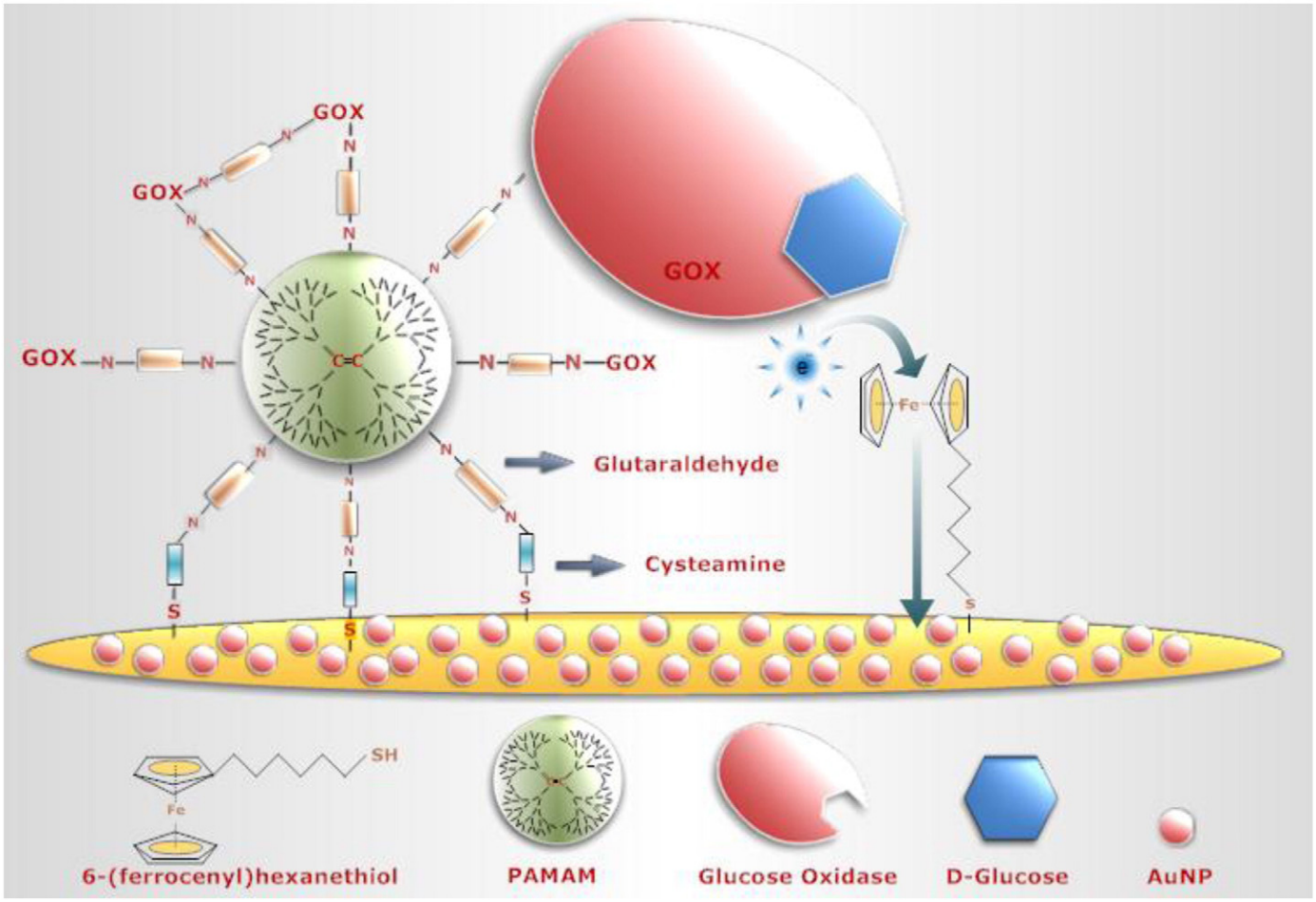

Scheme 1. Schematic representation of the proposed biosensor.

Additionally, to monitor the morphology of the gold surface after modification with AuNP (A) and AuNP/FcSH (B) AFM was used in non-contact mode. The difference between the surfaces after each modification could be easily seen in Fig. 2. Cyst/PAMAM and Cyst/PAMAM/Enzyme modified gold electrodes were investigated in our previous work in which layer by layer formation of the immobilization matrices was examined as the alcohol sensing system [22].

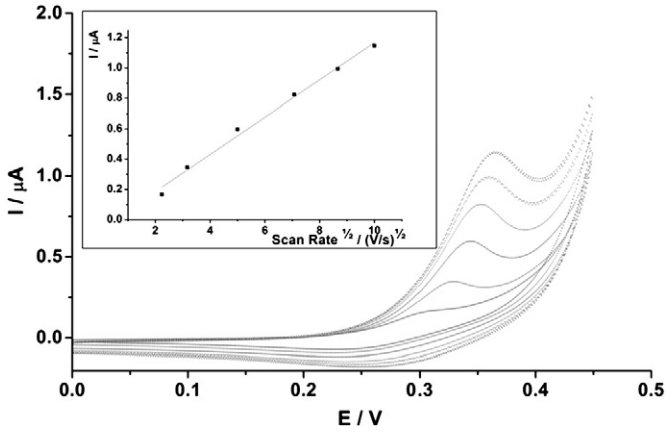

Fig. 1. Cyclic voltammograms of Au/(FcSH + Cyst)/PAMAM/AuNP/GOx biosensor (50 mM, pH 4.0 acetate buffer; 5.0 µL AuNPs; 1.98 µmol FcSH; 42 U GOx; scan rates in the range of 5.0–100 mV s^{-1}). Scan rates are 5.0, 10, 25, 50, 75, 100 mV/s from inside to out.

3.2. Optimization studies

The medium pH is an influential parameter for enzymes to keep their activity and catalysis efficiency. The optimum pH of GOx enzyme in soluble form was established as 5.5–6.0 [23]. On the other hand, it is known that immobilized enzyme could exhibit a shift in optimum pH depending on the selected immobilization matrices. The alteration on optimum pH has been reported for GOx previously [24]. An immobilized form it depends on the acidic character of other groups on the electrode surface and amino bearing groups tend to shift this optimum pH to more acidic region. In fact, in this case the maximum response of Au/AuNP/(FcSH + Cyst)/PAMAM/GOx has shifted to more acidic pH in agreement with the general observation that the positively-charged supports displace pH-activity curves of the enzymes attached to them towards lower pH values [25,26]. Fig. 3 shows the dependence of the signal of Au/AuNP/(FcSH + Cyst)/PAMAM/GOx to glucose in various pHs between 3.0 and 4.5. Maximum response was obtained at pH 4.0 and this effect has been observed also in our previous study [22].

The effect of enzyme loading on the biosensor response was examined using a different amount of GOx in the bioactive layer. 1.0, 2.0 and 3.0 mg of enzymes solved in 5.0 µL potassium phosphate buffer (pH 7.0; 50 mM), corresponding to 21, 42 and 63 U GOx activity on the electrode surface. Fig. 4 shows the variations of the signals as a function of GOx loading. The biosensor response increased proportionally with the enzyme loading up to 42 U. Higher amounts of GOx results in a decline in the response signal probably due to the difficulties in diffusion of the substrate in thick biocomponent surface.

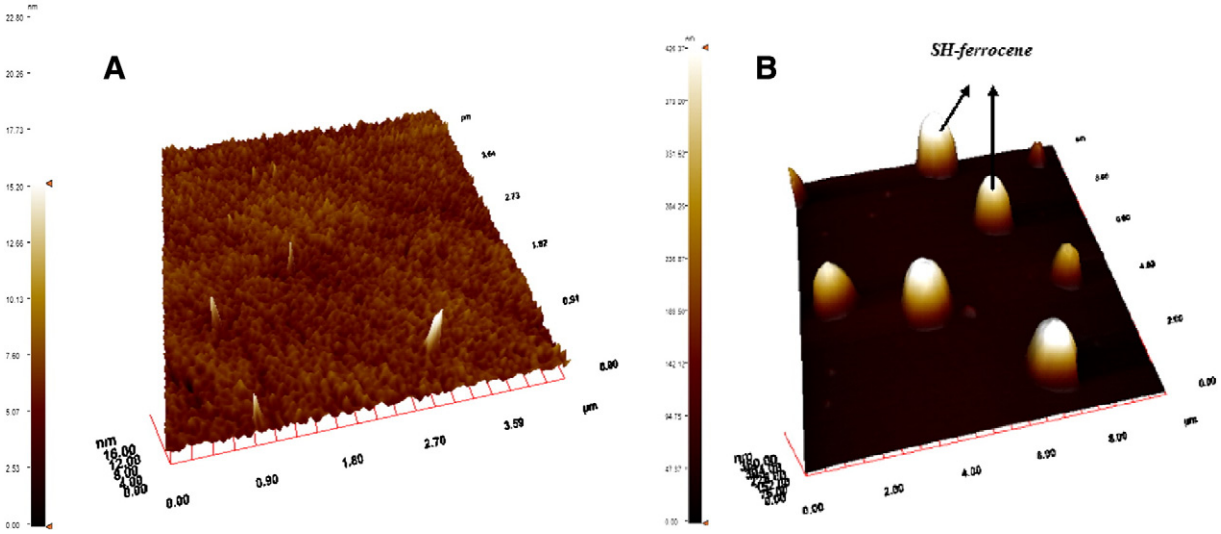

Fig. 2. AFM images of AuNP modified (A) and AuNP/SH-ferrocene modified (B) gold surface.

The effect of FcSH amount was also investigated and as shown in Fig. 5, maximum biosensor response was obtained by using 1.98 μmol FcSH in the electrode configuration. This value was used in further studies. Higher amounts of FcSH have led a decline in biosensor response due to the competitive adsorption with not only cysteamine but also with gold nanoparticles for active sites of the surface.

AuNPs provide a stable immobilization of biomolecules and retaining their bioactivity is a major advantage for the preparation of biosensors. The conductivity properties of AuNPs enhance the electron transfer between the active centres of proteins and electrodes and thus they act as electron transfer "electron wires" [27]. These particles also permit direct electron transfer between redox proteins and bulk electrode materials [28]. One more thing to consider using AuNPs in biosensors is the catalytic properties which can decrease overpotentials of many analytically important electrochemical reactions [27]. The contribution of AuNPs in biosensor response was initially tested in the absence and presence of AuNPs in construction. Fig. 6 clearly demonstrates a negative shift in peak potentials and a significant increase in peak current in the presence of AuNPs. This might be due to the presence of AuNPs in contact with enzyme which improves the electron transfer between redox species and catalytic centre of the enzyme.

Alternatively, GOx was incubated with AuNPs for 30 min before dropping the electrode surface. Responses obtained was far lower with linear regression equation $y = 0.0007x - 0.0012$, $R^2 = 0.961$ in contrast the electrode used in this study ($y = 0.01x - 0.004$, $R^2 = 0.992$).

Additionally, to study their influence on the performance of GOX biosensor, a series of biosensors were prepared with different amounts of AuNPs and calibration plots for glucose were obtained for each biosensor (Fig. 7).

Clearly, amperometric results have shown that using AuNPs enhances the biosensor response up to a point and then, shows a decline in response. The reason behind this might be diffusion limitations caused by excessive amount of gold suspension used.

3.3. Analytical characteristics

The response of the biosensor as a function of the glucose concentration was studied using +0.35 V as the working potential, 50 mM acetate buffer (pH 4.0) as the working buffer. A linear relationship between the concentration and the current was obtained for glucose in

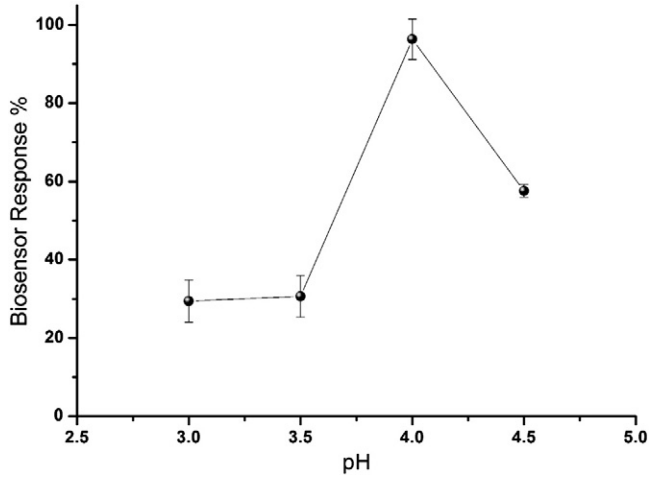

Fig. 3. Effect of pH (50 mM acetate buffers in the range of pH 3.0–4.5; +0.35 V, 2.5 mM glucose).

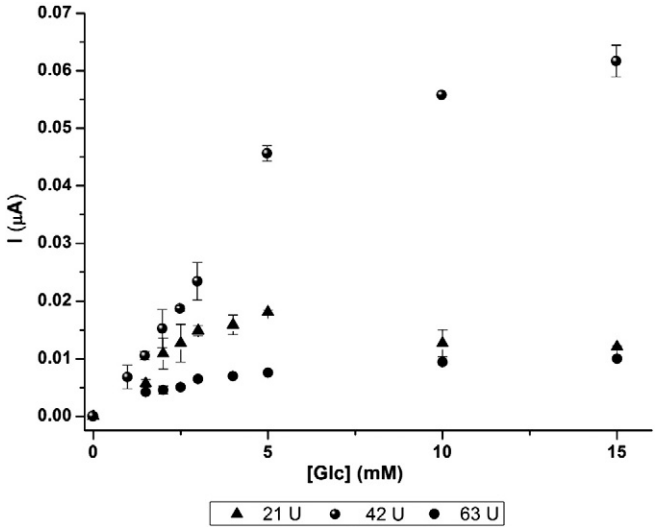

Fig. 4. Effect of enzyme loading on the biosensor response (50 mM, pH 4.0 acetate buffer; 5.0 μL AuNPs; 1.98 μmol FcSH; +0.35 V).

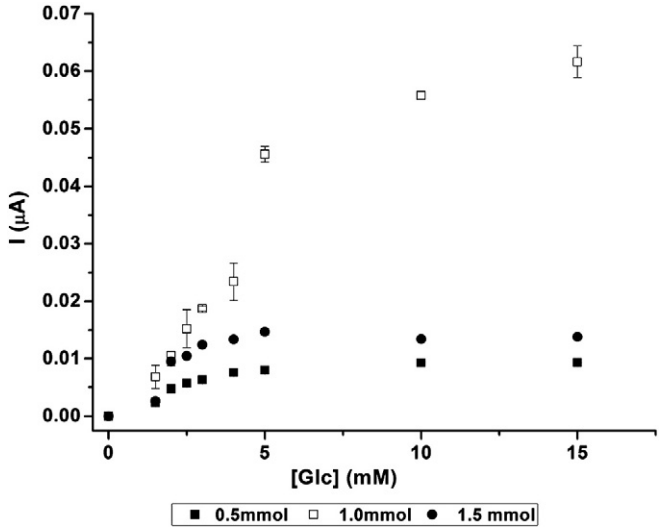

Fig. 5. Effect of the FcSH amount on the biosensor response studied by calibration plots obtained for glucose (50 mM pH: 4.0 acetate buffer; 5.0 μL AuNPs; 42 U GOx; +0.35 V).

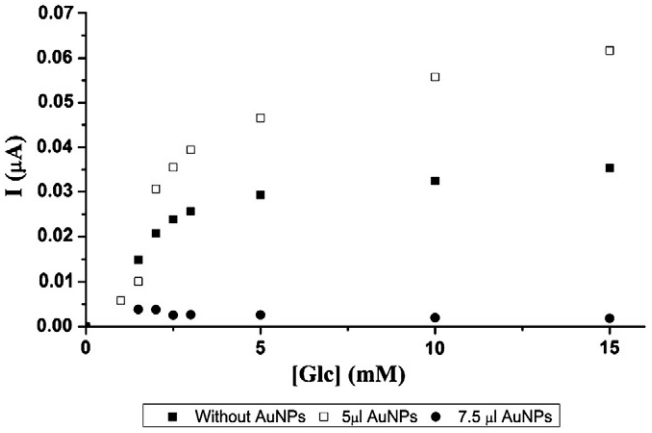

Fig. 7. Effect of the AuNPs amount on the biosensor response in 50 mM, pH 4.0 acetate buffer (1.98 μmol FcSH; 42 U GOx; +0.35 V).

the 1.0–5.0 mM range and described by the equation of $y = 0.01x - 0.004$ ($R^2 = 0.992$), (Fig. 8).

Repeatability of the response among measurements is important in fabrication of biosensor. For this aim, intra-day variation coefficient (cv, %) and relative standard deviation (RSD) were observed as 4.8% and ±0.013 for the eight successive measurements of 2.5 mM glucose.

The fabrication conditions of the electrode might also affect the precision. The reproducibility was calculated with three independent biosensors by measuring the current responses to 2.0 and 2.5 mM glucose at the optimised working conditions, and 3.1% and 1.2% RSD were obtained respectively. Similarity in the slope of plots (Fig. 9) for different biosensors and RSD values indicate good reproducibility for proposed biosensor.

The operational stability of the proposed sensors under optimized conditions was tested for 3 h. When the electrode was placed in working buffer at 25 °C and measured intermittently, no apparent changes in the response to 4.0 mM glucose was observed for first 2.5 h, and 92% of the response was retained for 3 h, with the Au/AuNP/(FcSH + Cyst)/PAMAM/GOx biosensor.

Shelf life of the proposed biosensor was determined by measurements per day for a week. 2 mM glucose was used for shelf life studies and biosensor is kept at working buffer solution at 4 °C when not in use. Biosensor retained 89.2% activity after 7 days.

Analytical characteristics of various glucose biosensors prepared with other approaches in the literature have been briefly presented in Table 1 and compares the proposed biosensor.

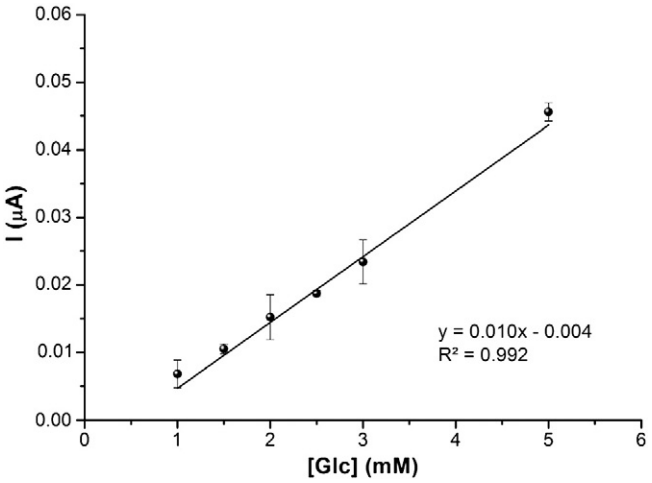

Fig. 8. Calibration plot for glucose in optimized conditions (50 mM, pH 4.0 acetate buffer; 5.0 μL AuNPs; 1.98 μmol FcSH; 42 U GOx; +0.35 V).

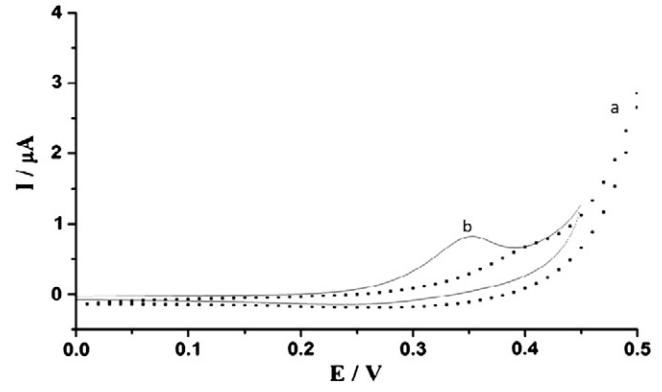

Fig. 6. Voltammograms comparing electrodes in absence (a) and presence of AuNPs (5.0 μL) (b) in 50 mM pH 4.0 acetate buffer (1.98 μmol FcSH; 42 U GOx; scan rate: 50 mV s^{-1}).

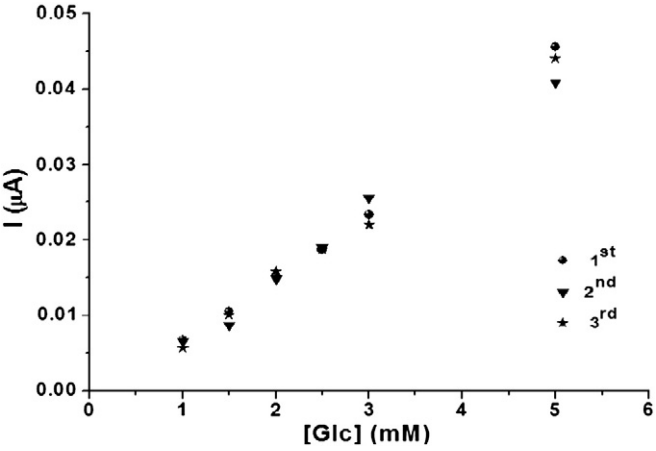

Fig. 9. Calibration plots of three different biosensor prepared on different days (50 mM pH 4.0 acetate buffer; 5.0 μL AuNPs; 1.98 μmol FcSH; 42 U GOx; +0.35 V).

Table 1
Comparison of performances of various glucose biosensors in literature.

Configuration	Operational stability	Linear range	Limit of detection	Working potential (vs. Ag/AgCl)	Real samples	Reference
(AuNP–PANI)/AgCl/ Gelatin/ PyOx	88% (6 h)	0.05–0.75 mM	n.r.	−0.7 V	Pomegranate juice, green tea, energy drink, raspberry nectar, peach juice, orange juice, mixed fruit juice, coke, wine	[29]
(CHIT–Fc)/GOx	87% (7.2 h)	0.8–4.0 mM	0.565 mM	+0.35 V	Coke, cherry juice	[30]
(SNS-NH_2–CNT)/ AuNP/GOx	84% (6 h)	0.05–0.75 mM	2.1 μM	−0.7 V	Fizzy, coke, peach juice, lemonade, ice tea, peach juice, orange juice, green tea	[31]
(Fe_3O_4–SiO_2)/GOx	83% (6 h)	0.25–2.0 mM	n.r.	−0.7 V	Green tea, lemonade, ıce tea, peach juice, orange juice, mixed fruit juice, sour cherry juice, coke, fizzy	[32]
Cyst/PAMAM/PyOx	100% (8 h)	0.025–0.5 mM	7.45 μM	−0.7 V	Fermentation medium (*Saccharomyces cerevisiae* H620)	[33]
Cyst/PAMAM/GOx	100% (8 h)	0.01–1.0 mM	11.84 μM			
PBDT/GOx	n.r.	0.05–2.0 mM	0.05 mM	−0.7 V	Human serum samples	[34]
PESeE/GOx		0.01–2.0 mM	0.01 mM			
PMMA–BSA/GOx	93.7% (50 successive scans)	0.2–9.1 mM	n.r.	+0.4 V	Human serum samples	[35]
DM-Mont/GOx	n.r.	0.05–1.0 mM	0.038 mM	−0.7 V	White Wine	[36]
DM-Mont/Gox (FIA)	100% (75 injections in 130 min)	1.0–10.0 mM	0.47 mM			
Pt-DENs /PANI/CNT/ GOx	n.r.	1.0 μM–12 mM	0.5 μM	0.0 V	n.r.	[37]
CHIT-CNT/GOx	n.r.	1.0–10 mM	21 μM	+0.6 V	n.r.	[38]
Osmium redox polymer/ PyOx	88% (6 h)	0.25 – 6.0 mM	n.r.	+0.3 V	n.r.	[39]
AuNP/ (FcSH + Cyst)/PAMAM /GOx	100% (2.5 h) 92% (3 h)	1.0–5.0 mM	0.6 mM	+0.35 V	Cherry juice, fizzy with orange	This work

AuNPs: gold nanoparticles; PANI: polyaniline; PyOx: pyranose oxidase; CHIT: chitosan; Fc: ferrocen; GOx: glucose oxidase ; SNS–NH_2: 4-(2,5-di(thiophen-2-yl)-1 H-pyrrole-1-l) benzenamine; CNT: carbon nanotube; PBDT: poly(4,7-di(2,3)-dihydrothienol[3,4-b][1,4]dioxin-5-yl-benzo[1,2,5]thiadiazole); PESeE: poly(4,7-di(2,3)-dihydrothienol[3,4-b][1,4] dioxin-5-yl-2,1,3-benzoselenadiazole; PMMA: poly(methyl methacrylate); BSA: bovine serum albumin; Pt-DENs: dendrimer-encapsulated Pt nanoparticles; FcSH: 6-(ferrocenyl) hexanethiol; Cyst: cysteamine; PAMAM: poly(amido amine).

Table 2
Results for glucose analysis in real samples by of PAMAM/AuNPs/FcSH/GOx biosensor and HPLC.

Sample	Glc (g/100 mL)*		Recovery (%)
	Biosensor	HPLC	
Cherry juice	6.33 ± 0.629	6.03 ± 0.121	105
Fizzy with orange	4.44 ± 0.176	4.76 ± 0.069	93

* Data were calculated as the average of 3–5 trials ± S.D.

3.4. Sample application

The Au/AuNP/(FcSH + Cyst)/PAMAM/GOx biosensor was applied to the determination of glucose content in some commercial beverages and the results obtained were compared with those from HPLC. Glucose standard curve obtained from the HPLC was defined by the equation of $y = 135042x - 1478.6$ ($R^2 = 0.999$), in which x and y show glucose concentration in mg/mL and peak area; nano Refractive Index Unit (corresponds to the difference between the refractive index of sample in the sample cell and the mobile phase in the reference cell in HPLC system, nRIU), in the range of 0.25–1.0 mg/mL glucose. The comparison of the results obtained from both HPLC and Au/AuNP/(FcSH + Cyst)/ PAMAM/GOx biosensor was shown in Table 2 and according to data it can be said that the use of Au/AuNP/(FcSH + Cyst)/ PAMAM/GOx biosensor resulted in very similar results in compared to the HPLC. Satisfactory recovery values were obtained based on the HPLC results.

4. Conclusions

Present work describes development of an electrochemical Au/AuNP/(FcSH + Cyst)/PAMAM/GOx biosensor. The concentration of glucose was quantified according to the determination of the oxidation signal of FcSH on the surface of PAMAM/AuNPs modified gold electrodes. After optimization and characterization studies, the biosensor developed was adopted to glucose determination in real samples. The results were compared with those of HPLC method and quite similar results were obtained. In future studies, the prepared Au/AuNP/(FcSH + Cyst)/PAMAM/GOx biosensor can be applied in various biotechnological applications such as analytical applications as well as enzymatic biofuel cell applications.

Acknowledgements

The authors acknowledge the financial support from the Ege University Research Fund (project number: 2011 FEN 039).

References

[1] L.C. Clark Jr., C. Lyons, Ann. N. Y. Acad. Sci. 102 (1962) 29–45.
[2] J.W. Li, J.J. Yu, F.Q. Zhao, B.Z. Zeng, Anal. Chim. Acta 587 (2007) 33–40.
[3] J. Wang, Electroanalytical 13 (2001) 983–988.
[4] A. Chaubey, B.D. Malhotra, Biosens. Bioelectron. 17 (2002) 441–456.
[5] T. Kuwahara, H. Ohta, M. Kondo, M. Shimomura, Bioelectrochemistry 74 (2008) 66–72.
[6] S.X. Zhang, N. Wang, Y.M. Niu, C.Q. Sun, Sens. Actuators, B 109 (2005) 367–374.
[7] L. Svobodova, M. Snejdarkova, T. Hianik, Anal. Bioanal. Chem. 373 (2002) 735–741.
[8] S. Rubin, G. Bar, R.W. Cutts, J.T. Chow, J.P. Ferraris, T.A. Zawodzinski, Mater. Res. Soc. Symp. Proc. 413 (1996) 377–388.
[9] X. Yao, M.L. Yang, Y.F. Wang, Z.B. Hu, Sens. Actuators, B 122 (2007) 351–356.
[10] L.A. Bauer, N.S. Birenbaum, G.J. Meyer, J. Mater. Chem. 14 (2004) 517–526.
[11] X.L. Luo, A. Morrin, A.J. Killard, M.R. Smyth, Electroanalytical 18 (2006) 319–326.
[12] H.M.E. Azzazy, M.M.H. Mansour, S.C. Kazmierczak, Clin. Chem. 52 (2006) 1238–1246.
[13] K.K. Jain, Clin. Chem. 53 (2007) 2002–2009.
[14] J.R. Chen, Y.Q. Miao, N.Y. He, X.H. Wu, S.J. Li, Biotechnol. Adv. 22 (2004) 505–518.
[15] D. Hernandez-Santos, M.B. Gonzalez-Garcia, A.C. Garcia, Electroanalytical 14 (2002) 1225–1235.
[16] W.W. Yang, J.X. Wang, S. Zhao, Y.Y. Sun, C.Q. Sun, Electrochem. Commun. 8 (2006) 665–672.
[17] S.X. Zhang, N. Wang, H.J. Yu, Y.M. Niu, C.Q. Sun, Bioelectrochemistry 67 (2005) 15–22.
[18] M. Snejdarkova, L. Svobodova, V. Gajdos, T. Hianik, J. Mater. Sci. - Mater. Med. 12 (2001) 1079–1082.
[19] Z.M. Liu, Y. Yang, H. Wang, Y.L. Liu, G.L. Shen, R.Q. Yu, Sens. Actuators, B 106 (2005) 394–400.
[20] M. Snejdarkova, L. Svobodova, D.P. Nikolelis, J. Wang, T. Hianik, Electroanalytical 15 (2003) 1185–1191.

[21] E. Laviron, J. Electroanal. Chem. 101 (1979) 19–28.
[22] M. Akin, M. Yuksel, C. Geyik, D. Odaci, A. Bluma, T. Hopfner, S. Beutel, T. Scheper, S. Timur, Biotechnol. Progr. 26 (2010) 896–906.
[23] E. Raabe, L. Kroh, J. Vogel, J. Biochem. Bioph. Methods 29 (1994) 207–216.
[24] J. Yu, S. Liu, H. Ju, Biosens. Bioelectron. 19 (2003) 401–409.
[25] M.A. Abdel-Naby, A.A. Sherif, A.B. El-Tanash, A.T. Mankarios, J. Appl. Microbiol. 87 (1999) 108–114.
[26] B. Krajewska, M. Leszko, W. Zaborska, J. Chem. Technol. Biotechnol. 48 (1990) 337–350.
[27] S.Q. Xu, Y.Y. Li, H.J. Schluesener, Gold Bull. 43 (2010) 29–41.
[28] J.M. Pingarron, P. Yanez-Sedeno, A. Gonzalez-Cortes, Electrochim. Acta 53 (2008) 5848–5866.
[29] C. Ozdemir, F. Yeni, D. Odaci, S. Timur, Food Chem. 119 (2010) 380–385.
[30] Ö. Yılmaz, D.O. Demirkol, S. Gülcemal, A. Kılınç, S. Timur, B. Çetinkaya, Colloids Surf., B 100 (2012) 62–68.
[31] S. Tuncagil, C. Ozdemir, D.O. Demirkol, S. Timur, L. Toppare, Food Chem. 127 (2011) 1317–1322.
[32] C. Ozdemir, O. Akca, E. Medine, D. Demirkol, P. Unak, S. Timur, Food Anal. Methods 5 (2012) 731–736.
[33] M. Yuksel, M. Akin, C. Geyik, D.O. Demirkol, C. Ozdemir, A. Bluma, T. Hopfner, S. Beutel, S. Timur, T. Scheper, Biotechnol. Progr. 27 (2011) 530–538.
[34] F.B. Emre, F. Ekiz, A. Balan, S. Emre, S. Timur, L. Toppare, Sens. Actuators, B 158 (2011) 117–123.
[35] C. He, J. Liu, Q. Zhang, C. Wu, Sens. Actuators, B 166–167 (2012) 802–808.
[36] M. Seleci, D. Ag, E.E. Yalcinkaya, D.O. Demirkol, C. Guler, S. Timur, RSC Adv. 2 (2012) 2112–2118.
[37] L. Xu, Y. Zhu, X. Yang, C. Li, Mater. Sci. Eng., C 29 (2009) 1306–1310.
[38] B.-Y. Wu, S.-H. Hou, M. Yu, X. Qin, S. Li, Q. Chen, Mater. Sci. Eng., C 29 (2009) 346–349.
[39] S. Timur, Y. Yigzaw, L. Gorton, Sens. Actuators, B 113 (2006) 684–691.